

DISCLAIMER

This work was sponsored by the Office of Naval Research, Office of Naval Research, Department of the Navy, under Grant N00019-79-1-0001. The views and conclusions contained herein are those of the author and do not necessarily reflect those of the Office of Naval Research, Department of the Navy. This work was also supported by the Office of Naval Research, Office of Naval Research, Department of the Navy, under Grant N00019-79-1-0001. The views and conclusions contained herein are those of the author and do not necessarily reflect those of the Office of Naval Research, Department of the Navy.

RF ENERGY COMPRESSOR*

Z. D. Farkas
Stanford Linear Accelerator Center
Stanford University, Stanford, California 94305

CONF-8005100 1
MASTER

Abstract

The RF Energy Compressor, REC described here, transforms cw rf into periodic pulses using an energy storage cavity, ESC, whose charging and discharging is controlled by 180° M-phase modulation, PSK, and external Q switching, Q_e . Compression efficiency, C_c , of 100% can be achieved for any compression factor C_f .

Introduction

There are many applications where we need a train of rf pulses, each pulse containing a given energy over a given time such as for charged particle accelerators, for radar and for communication. Usually the energy is built up during the time between pulses in a capacitor which discharges into an rf tube that converts the dc energy into rf. The REC performs a similar task, but it stores rf instead of dc energy. Just like a capacitor in a hard tube modulator, the ESC acts as a fly-wheel. It takes energy in between pulses and delivers it during the pulse. The control that tells the ESC when to accept and when to deliver energy is a π power 180° M-phase modulator. The energy is delivered at a rate determined by a switch that controls the effective size of the cavity opening, i.e., its external Q. We arrange the duration and rate of ESC charging and discharging such that average energy level in the cavity is such that during charging, it accepts all the generator energy available and during discharging, delivers it, together with the generator energy available during discharge, into a load.

Theory

The differential equation that governs the emitted field amplitude of a tuned cavity with an incident field E_i is¹

$$T_c (dE_c/dt) + E_c = aE_i \quad (1)$$

$B = Q_0/Q_e$, $a = 2B/(1+B)$, $T_{C0} = Q_0/\omega$, $T_c = T_{C0}/(1+B)$ where B is the coupling factor, the ratio of emitted to dissipated power, ω is the steady state emitted field, T_c is the cavity time constant, Q_0 is the unloaded Q factor, T_{C0} is the unloaded cavity time constant. Its solution during a time interval t_n , during which T_c and E_i are constant is

$$E_{ent} = E_{enf} + [E_{eni} - E_{enf}] e^{-t/T_n} \quad (2)$$

where

E_{ent} = the emitted field at the end of time interval t_n ,

E_{enf} = the steady state emitted field, the emitted field that would have been reached if t_n were infinite = aE_i ,

E_{eni} = the emitted field at the beginning of interval t_n ,

T_n = the normalized duration of the nth interval = t_n/T_{C0} .

If we have a given E_{iA} and Q_{eA} during interval 'a' and E_{iB} and Q_{eB} during the next interval 'b' and this interval pair repeats indefinitely, then the initial and final emitted fields during the two intervals are:

$$E_{eA} = E_{eAf} + [E_{eAi} - E_{eAf}] e^{-T_A} \quad (3)$$

$$E_{eB} = E_{eBf} + [E_{eBi} - E_{eBf}] e^{-T_B} \quad (4)$$

Using $E_{eAi} = E_{eAf}$ and $E_{eBi} = E_{eBf}$ in Eq. (3) and (4) and noting that E_c does not change during transition and $E_{eAf} = E_{eBf}$ and $E_{eBf} = E_{eAf} e^{-T_B}$, we obtain

$$E_{eAf} = E_{eAf} + [(1/T_A) e^{-T_A} - 1] E_{eAf} T_A \quad (5)$$

$$E_{eBf} = E_{eBf} + [(1/T_B) e^{-T_B} - 1] E_{eBf} T_B \quad (6)$$

where $\lambda = (T_c/Q_0)^2 + (T_c/Q_{e0})^2$. Solving Eqs. (5) and (6) simultaneously and using $E_{eBf} = E_{eAf} e^{-T_B}$ we obtain

$$E_{eAf} = \frac{E_{eAf} (1 - e^{-T_A}) + (1/\lambda) e^{-T_A} (1 - e^{-T_B})}{1 - e^{-T_A}} \quad (7)$$

$$E_{eBf} = \frac{E_{eBf} (1 - e^{-T_B}) + (1/\lambda) e^{-T_B} (1 - e^{-T_A})}{1 - e^{-T_B}} \quad (8)$$

Using $E_{eAf} = E_{eBf} e^{-T_B}$ and $E_{eBf} = E_{eAf} e^{-T_A}$ we obtain $E_{eAf} = (1/\lambda) e^{-T_A} (1 - e^{-T_B}) / (1 - e^{-T_A} - e^{-T_B})$ and $E_{eBf} = (1/\lambda) e^{-T_B} (1 - e^{-T_A}) / (1 - e^{-T_A} - e^{-T_B})$. The field transmitted into the cavity from a generator with a constant flux E_{i0} is the steady state value of the reflected field. Hence $E_{eAf} = E_{eBf} = E_{i0} (1 - e^{-T_A} - e^{-T_B}) / (1 - e^{-T_A} - e^{-T_B})$. Thus, by using the external Q condition, we have solved for all the steady state parameters of the REC as they are given in Table I, respectively. An excellent review of this theory is given in Ref. 2.

Generator and Load

Define the modulation index M as the ratio of the compression factor, $C_f = E_{eAf}/E_{i0}$, to the average incident field, which is the normalized average incident field,

$$\text{by the period, } T_c = 1/\omega \int_0^{T_c} E_{i0} dt = T_c E_{i0} = (E_{eAf} + E_{eBf}) e^{-T_B} T_c \text{ we can calculate } C_f \text{ and } M \text{ as in Eqs. (2), (3), (8).}$$

To get insight and appreciation of the results, let us for C_f as a function of T_A and T_B and λ we will consider the limiting case $\lambda \rightarrow 0$, i.e., $T_c \rightarrow 0$. Then, $E_{eAf} = E_{eAf} + [E_{eAi} - E_{eAf}] e^{-T_A} = E_{eAf}$, $E_{eBf} = E_{eBf} + [E_{eBi} - E_{eBf}] e^{-T_B} = E_{eBf}$, $E_{eAf} = 2E_{eBf} e^{-T_B}$, $C_f = 2E_{eBf} e^{-T_B} / E_{i0} = 2E_{i0} (1 - e^{-T_A} - e^{-T_B}) / (1 - e^{-T_A} - e^{-T_B}) = 2(1 - e^{-T_A} - e^{-T_B}) / (1 - e^{-T_A} - e^{-T_B}) = 2$. If we set $T_A = T_B = T$, $C_f = 2(1 - e^{-T} - e^{-T}) / (1 - e^{-T} - e^{-T}) = 2(1 - 2e^{-T}) / (1 - 2e^{-T}) = 2$. If $T_A = 0$, $E_{eAf} = E_{eAf} + [E_{eAi} - E_{eAf}] e^{-T_A} = E_{eAf}$, $E_{eBf} = E_{eBf} + [E_{eBi} - E_{eBf}] e^{-T_B} = E_{eBf}$, $E_{eAf} = E_{eBf}$, $C_f = (E_{eAf} + E_{eBf}) e^{-T_B} / E_{i0} = 2E_{eAf} e^{-T_B} / E_{i0} = 2E_{i0} (1 - e^{-T_A} - e^{-T_B}) / (1 - e^{-T_A} - e^{-T_B}) = 2(1 - e^{-T_A} - e^{-T_B}) / (1 - e^{-T_A} - e^{-T_B}) = 2$. If $T_B = 0$, $E_{eAf} = E_{eAf} + [E_{eAi} - E_{eAf}] e^{-T_A} = E_{eAf}$, $E_{eBf} = E_{eBf} + [E_{eBi} - E_{eBf}] e^{-T_B} = E_{eBf}$, $E_{eAf} = E_{eBf}$, $C_f = (E_{eAf} + E_{eBf}) e^{-T_B} / E_{i0} = 2E_{eAf} e^{-T_B} / E_{i0} = 2E_{i0} (1 - e^{-T_A} - e^{-T_B}) / (1 - e^{-T_A} - e^{-T_B}) = 2(1 - e^{-T_A} - e^{-T_B}) / (1 - e^{-T_A} - e^{-T_B}) = 2$. We can observe the proper λ and obtain 100% conversion efficiency. It turns out that not only does the above relationship between C_f and M with $C_f = 100%$ at ideal

* Work supported by the Department of Energy, contract DE-AC-3-78SF00515.

EB

conditions but also yields maximum efficiency when C_f is considerably less than 100%.

The maximum efficiency for the nonideal case is obtained as follows. For a given t_0 , C_f , T_{CO} there is a unique value of β_0 that maximizes C_e . If β_0 is too large, then T_{CO} is too small and a large fraction of the charging energy is reflected; if it is too small then a large fraction of the charging energy is dissipated in the cavity and α_0 is too small. Plots of C_e vs. β_0 for several values of T_{CO} and for $C_f = 10$ are shown in Fig. 3. The curves are nearly independent of C_f . Figure 4 is a plot of C_e vs. T_{CO} with β_0 optimized for maximum conversion efficiency. As C_f increases above its optimum value, P_p increases but at a slower rate than C_f to a limiting value of $k_0 + 1$. Thus, C_e decreases first slowly and in the limit of large C_f , inversely as C_f . The curves of Fig. 5 are plots of C_e and P_p vs. C_f normalized to $C_f = (1+k)^2 = C_{f0}$, for which $C_e = 1$ under ideal conditions. The points shown were experimentally obtained.

If, during t_0 , the incident field is turned off instead of shifted 180° we have β_0 only and $E_{0bf} = 0$ instead of α_0 . Then, the ideal gain is $C_f - 1$ which can be approached if $C_f = 1+k^2$. The bottom two curves of Fig. 5 are plots of C_e and P_p for β_0 only. The points shown were experimentally obtained.

Practical Considerations

The period is given by:

$$t_2 = t_0 T_{CO} = t_0 Q_0 / \pi f = t_0 \omega / \pi R_{s0} \pi f$$

Γ is the cavity geometric factor which depends only on cavity geometry and not on R_{s0} . $R_{s0} = 2.61 \times 10^{-8}$ is the operating frequency in MHz. The surface resistance of a niobium cavity operating at liquid helium temperature, 4.2°K, $R_{s0} = R_0 \cdot 10^{-9} f^{3/2}$. If we use a TE₀₁₃ cavity for the ESC and we accept an efficiency of 80%, then $\Gamma = 780$ and from Fig. 4, $t_0 = 90 \times 10^{-7}$. Thus, with a copper ESC the maximum t_2 is 0.36 μ s. and with a superconducting ESC it is 3.7 μ s. Using TE₀₂₃ spherical cavities, such as used by Ray Alvarez at Lawrence Livermore Laboratories, Γ , and hence t_2 is increased by a factor of five.

The minimum pulse width, t_1 , which determines the maximum C_f for a given period, is determined by the speed of PSK and β_0 switches. The maximum power output depends on the power handling ability and the maximum period on the minimum dissipation of the β_0 . Birk and Scallapino have reported a high intensity electron beam switch which can function in an evacuated x-band superconducting waveguide.² They obtained Q_0 ratios of 4×10^3 and T_{CO} of 500 μ s. Using an electron beam is analogous to a hard tube modulator. However, it can be much simpler because it does not require to hold off the high power amplifier voltage, and to carry the amplifier current.

The PSK switch does not limit output power because the power amplifier is interspersed between the PSK switch and the ESC as shown in Fig. 6, so that the PSK switch operates at low power. Thus, for C_f approximately four, only low power switches are required. If $C_f = 4$ then $k = 1$ and, therefore, for this special case we approach 100% compression efficiency without β_0 -switching, using PSK only. At the Stanford Linear Accelerator Center (SLAC) using single pulse PSK, and TE₀₁₃ ESC we have obtained output powers in excess of 125 MW. To illustrate the versatility of the NEC 122 list in the table below the parameters of the present and several REC modes of SLAC operation, if we keep the 114 kW AC power input but replace the 50% efficient 38.5 MHz, pulsed klystrons with 60% efficient 60% Q klystrons (assume 80% AC to DC efficiency), and install REC with niobium

ESC at 4.2 K. The values are calculated as follows.

$T_{CO} = 75$ ns, $T_{CO} = C_f / \omega = 13.3 / \text{PRF}$. Obtain C_e from plot of C_e vs. T_{CO} , Fig. 4. $P_p = 10^3 C_e \omega^2 (\text{PRF})^2 / \omega$, $V = 10(\text{PRF} \cdot 30.5)^2$. P_{in} is the cw klystron power in kW, PRF is the pulse repetition frequency in s^{-1} , PW (or t_0) is the pulse width in μ s, and V is the SLAC beam voltage. The peak current I_p , and average current I_a are limited either by 10% loading, $I = 2.86V$, or by cw beam breakup, $I = .4V$, or by 1.5 μ s pulse beam breakup, $I = 70V/24$. dc is the duty cycle.

| PRF 1/s | PW μ s | C_e | P_p MW | V GeV | I_p ma | I_a A | dc |
|-----------------|---------------|-------|-------------|----------|-------------|------------|------|
| 360 | 2.5 | — | 38.5 | 30 | 87 | 50 | .06 |
| 360 | 2.5 | .92 | 61 | 38 | 87 | 50 | .06 |
| 180 | 1 | .86 | 287 | 82 | 200 | 11 | .005 |
| 133 | .9 | .85 | 427 | 100 | 200 | 8 | .004 |
| cw | cw | — | .06 | 1.2 | 400 | 400 | 100 |
| 10 ³ | 2.5 | .99 | .24 | 2.4 | 7.0 | 1120 | 16 |
| 10 ⁴ | 2.5 | .98 | 2.35 | 7.4 | 21.6 | 345 | 1.6 |
| 10 ⁵ | 2.5 | .96 | 23 | 23 | 67 | 107 | .16 |

With REC we can attain higher peak power, duty cycle, and average current than without REC. REC can be installed where cw klystrons already exist, as in electron-positron storage rings, and increase the beam energy as the number of bunches in the ring decrease. It is possible to have relatively closely spaced two or more pulses, and consider t_0 as the sum of their widths, as long as in a super period the energy into the cavity is equal to the energy lost by it. It is also possible to have different length consecutive periods as long as for each period $C_f = (1+k)^2$.

A means has to be provided to separate the reverse and forward powers. The simplest way is to connect the generator, cavity, and load, each to one of the arms of a three-port circulator. A second method, which does not have the power limitations of the circulator is to connect the generator, two identical cavities and the load to consecutive ports of a 3-dB hybrid as shown in Fig. 6. A third method is to use a resonant ring.

Conclusion

It was shown that rf energy compression with a gain of four at compression efficiencies nearly 100% and up to a gain of eight with compression efficiencies above 60%, at power outputs in excess of 100 MW are possible, using a low power microwave switch whose insertion loss is of no consequence. At low power, high efficiencies and high compression ratios can be attained if we limit the period. To attain high compression factor at high power levels depends on further development of a low loss, fast turn-on turn-off high power microwave switch.

Acknowledgment

Thanks to D. L. Birk of Lawrence Livermore Laboratories for enlightening discussions.

References

- Z. D. Farkas et al., "SLED: A Method of Doubling SLAC's Energy," Proc. of 9th International Conf. on High Energy Accel., p. 576, May 1976.
- P. B. Wilson, "The Theoretical Surface Resistance for Superconducting Load and Niobium at High Frequencies," SLAC-TN-70-35, December 1970.
- D. L. Birk and D. J. Scallapino, "Microwave Energy Compression Using a High Intensity Electron Beam Switch," to be published in Applied Physics Letters, in 1980.

PORTIONS OF THIS REPORT ARE ILLISIBLE

IF LAC USERS CAN BE HELD RESPONSIBLE FOR THE BEST AVAILABLE COPY OF THIS REPORT, PLEASE CONTACT THE AVAILABILITY

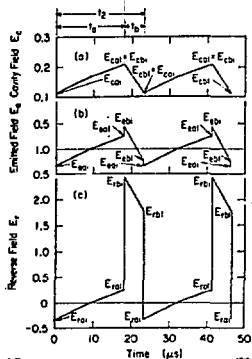


Fig. 1. REC fields vs time.

- (a) Cavity field, E_c .
 (b) Emitted field, E_e .
 (c) Reverse field, E_r .

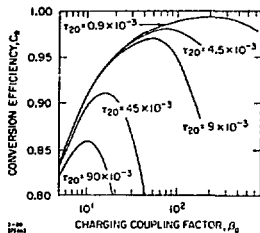


Fig. 3. Conversion efficiency, C_c , vs charging coupling factor, β_0 for several normalized period, τ_{20} .

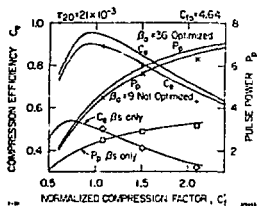


Fig. 5. Conversion efficiency C_c and normalized pulse power vs normalized compression factor, C_f .

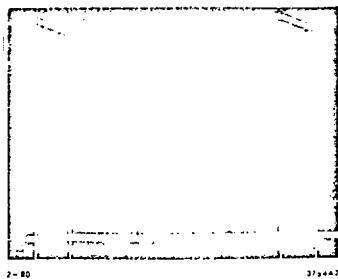


Fig. 2. Oscillogram of $|E_r|$ vs time (10 μ s/cm).

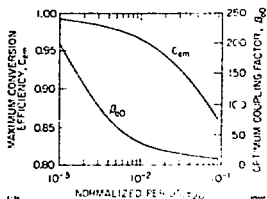


Fig. 4. Maximum C_c , C_m and optimum β_0 , τ_{20} vs normalized period, τ_{20} .

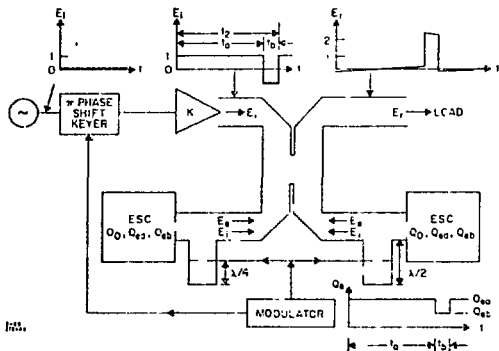


Fig. 6. RF energy compressor system.